



Fermi National Accelerator Laboratory

FERMILAB-Conf-99/128-E

D0 and CDF

Photon and Di-Photon Results from CDF and D0

Pierrick Hanlet

For the D0 and CDF Collaborations

*Northeastern University
Boston, Massachusetts 02115*

*Fermi National Accelerator Laboratory
P.O. Box 500, Batavia, Illinois 60510*

May 1999

Published Proceedings of the *13th Topical Conference on Hadron Collider Physics*,
Mumbai, India, January 14-20, 1999

Disclaimer

This report was prepared as an account of work sponsored by an agency of the United States Government. Neither the United States Government nor any agency thereof, nor any of their employees, makes any warranty, expressed or implied, or assumes any legal liability or responsibility for the accuracy, completeness, or usefulness of any information, apparatus, product, or process disclosed, or represents that its use would not infringe privately owned rights. Reference herein to any specific commercial product, process, or service by trade name, trademark, manufacturer, or otherwise, does not necessarily constitute or imply its endorsement, recommendation, or favoring by the United States Government or any agency thereof. The views and opinions of authors expressed herein do not necessarily state or reflect those of the United States Government or any agency thereof.

Distribution

Approved for public release; further dissemination unlimited.

Copyright Notification

This manuscript has been authored by Universities Research Association, Inc. under contract No. DE-AC02-76CHO3000 with the U.S. Department of Energy. The United States Government and the publisher, by accepting the article for publication, acknowledges that the United States Government retains a nonexclusive, paid-up, irrevocable, worldwide license to publish or reproduce the published form of this manuscript, or allow others to do so, for United States Government Purposes.

PHOTON AND DI-PHOTON RESULTS FROM CDF AND DØ

PIERRICK HANLET, FOR THE DØ COLLABORATION

Department of Physics, Northeastern University,

Boston, MA 02115, U.S.A.

E-mail: hanlet@fnal.gov

Measurements by the Fermilab DØ and CDF collaborations of prompt photon events in $p\bar{p}$ collisions at $\sqrt{s} = 1.8$ TeV are reported. The measured isolated photon cross sections are compared to current parton distribution functions and NLO QCD predictions. The cross section ratio of forward to central η bins and η distributions are presented and compared with theoretical predictions. $\gamma + 2jet$ events yield insight into final state radiation. A new measurement of $\gamma + \mu$ events is presented which probes the charm content of the proton. Finally, di-photon results are presented as a probe of initial state radiation; these results are compared to NLO QCD, Pythia parton showers, and resummation models.

1 Introduction

Since the late 1970's, it has been known that direct photons offer clean tests of Quantum Chromodynamics, QCD^{1,2}. At leading order in $p\bar{p}$ collisions, photons are produced in $q+g \rightarrow \gamma+q$ Compton scattering and $q+\bar{q} \rightarrow \gamma+g$ annihilation processes, thus providing direct probes of the partonic interactions without ambiguities associated with identification and measurement of jets, and/or with fragmentation.

Fig. 1 shows a typical Compton scattering event of two protons. Parton distribution functions, or *PDFs*, describe the initial states of the scattering partons; the hard scattering cross section, $\hat{\sigma}$, is calculated with next-to-leading-order (NLO) QCD. From the figure, one sees that a clean measurement of the prompt photon provides a direct probe of the interaction.

Also shown in the figure is a gluon radiated from the incoming proton due to the transverse momentum of the incoming partons. The soft, *intrinsic*, component of this transverse momentum due to the mass and the \sqrt{s} of the system is not described by perturbative QCD, *pQCD*; it therefore remains a topic of significant interest. Both photon and di-photon events are studied in hopes of offering insight into this process. The three theoretical and phenomenological models which attempt to describe this are parton showers³, resummation⁴, and k_T smearing⁵.

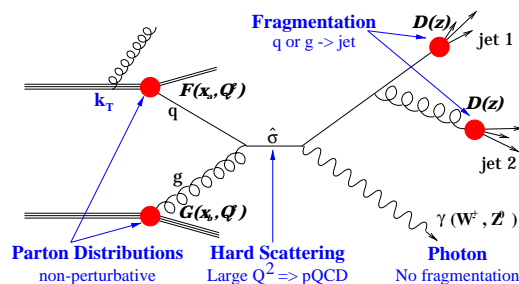


Figure 1. Example Compton scattering QCD event with prompt photon production

2 Data Analysis

2.1 Event Selection

Both DØ⁶ and CDF⁷ identified photons as isolated energy deposits in their electromagnetic (*EM*) calorimeters. Both experiments then applied selection cuts to their respective collected data sets to improve the signal-to-noise ratio in their photon candidate samples. These included fiducial cuts to ensure that showers were completely contained within active detector volumes, and background rejection cuts. Defining the pseudorapidity $\eta \simeq -\ln \tan(\frac{\theta}{2})$, where θ is the polar angle with respect to the proton beam, most of the analyses considered here required the photon candidates to be central with $|\eta| \leq 0.9$ and the interaction vertex to be near the center of the detectors. In addition, DØ applied an azimuthal cut to ensure contained showers in the central calorimeter region.

Background rejection required: (1) track rejection to ensure only neutral particles pointed to the shower; (2) a minimum fraction of the candidate shower's total energy be electromagnetic: 96% (89%) for DØ (CDF); (3) the candidates to be isolated from other energy deposits: $E_T^{iso} = E_T^{R < 0.4} - E_T^{R < 0.2} < 2$ GeV for DØ and $E_T^{iso} < 2$ GeV with $R < 0.7$ for CDF, where $R \equiv \sqrt{\Delta\eta^2 + \Delta\phi^2}$; (4) that the transverse shower profiles had acceptable shapes; and (5) a missing E_T cut to reject $W \rightarrow e\nu$ and cosmic ray events ($\cancel{E}_T < 20$ GeV for DØ and $\cancel{E}_T/E_T^2 < 0.5$ for CDF).

2.2 Photon Purity

These criteria reduced the data samples to events with candidates dominated by prompt photons and jets which fluctuated to single neutral mesons. At high enough E_T , the photons from these mesons coalesce to mimic single photons in the detectors. Since neither experiment could remove these candidates on an event-by-event basis, both experiments employed statistical methods to weight the events in a given bin by the probability that these candidates were single photons. In what follows, this probability is referred to as the photon purity which both experiments determine independently for each kinematic point.

DØ took advantage of the longitudinal segmentation of its calorimeter. Since the probability for one or more photons from a π^0 or η decay to convert is greater than that of a single photon, one expects more electrons, and hence more energy deposit in the first $2X_0$ longitudinal layer of the EM calorimeter, *EM1*. In short, background jets are expected to leave more energy in EM1 than prompt photons.

DØ modeled longitudinal energy depositions of γ 's and EM rich jets to perform a statistical comparison to data using the discriminant $\log(E_{EM1}/E_{total})$. Both signal and background energy depositions were simulated in Monte Carlo and the resulting normalized discriminants were fit to the data discriminant to determine the signal and background fractions in several E_T bins. As a check of the reliability of the Monte Carlo, distributions were compared with data $W \rightarrow e\nu$ event distributions and found to agree. Fig. 2 shows the photon purity as a function of E_T in both the central and forward regions of the detector.

In CDF, purities were determined using two discriminants: Shower Transverse Profile as determined using the Central Electromagnetic Strip chambers, or (*CES*), as compared to test beam electrons (used for low E_T); and Conversion Probability as determined using the Central Preradiator, or (*CPR*), (used for high E_T). The photon purity was then computed using $F = \frac{\epsilon - \epsilon_b}{\epsilon_\gamma - \epsilon_b}$, where ϵ is the photon candidate fraction passing the cuts as determined from data, ϵ_γ is the photon fraction for true photons, and ϵ_b is the background fraction; both ϵ_γ and ϵ_b are determined using Monte Carlo simulations to correct for the expected photon and background fractions. The corresponding values of ϵ , ϵ_γ , and ϵ_b for both the profile and conversion methods are shown in Fig. 3. As checks, the invariant masses of π^0 's, η 's, and ρ 's were measured, shower profiles were compared to test beam data, and profile and conversion methods were compared for consistency; in each case the results agreed with expectations.

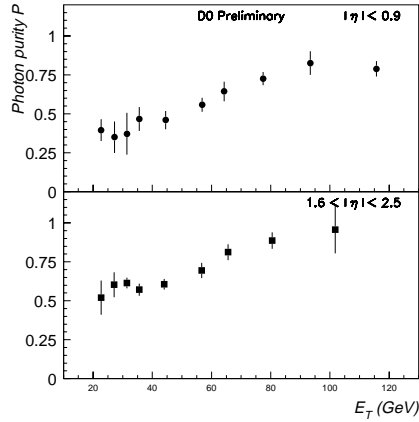


Figure 2. D0 photon purity: top is for the central region and the bottom is for the forward region.

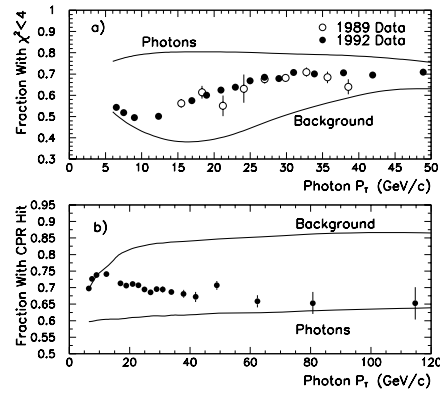


Figure 3. CDF photon fractions: top is the profile method using the CES, and bottom is using the conversion method with the CPR. In both plots, the top curve is the pure photon fraction, and the bottom is the pure background fraction.

3 Single Photon Results

3.1 Inclusive Photon Cross Sections

Both CDF and D0 have measured the photon inclusive cross section in the central region, $|\eta| \leq 0.9$; the results are shown in Fig. 4. The preliminary D0 result is from 95pb^{-1} of data taken in the 1994–1995 run. The CDF result⁸ is from $\sim 19\text{pb}^{-1}$ taken in the 1992–1993 run. The resulting cross sections are compared to NLO predictions of Baer, Ohnemus, and Owens with CTEQ4M parton distributions⁹ and a renormalization scale of $\mu = E_T^2$. The lower plot shows the same results on a linear scale. Here, the theoretical prediction is also compared to that using CTEQ2M¹⁰. The D0 inner error bars reflect the statistical error and outer error

bars the quadrature sum of statistical and systematic errors. The CDF error bars reflect statistical uncertainties, and the systematic errors are plotted as a band at the bottom. Both experiments are consistent, and are in agreement with theory for $E_T \gtrsim 30$ GeV, and both exhibit a rise above NLO QCD predictions at lower E_T .

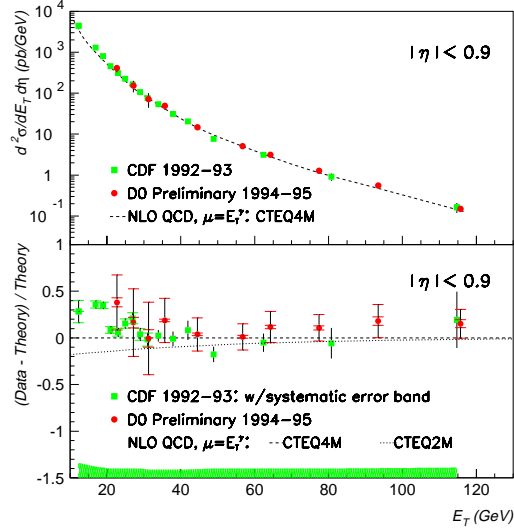


Figure 4. CDF/D0 Inclusive Photon Cross Section

3.2 Forward Photons

The D0 measurement¹¹ of the ratio Forward/Central Photon cross sections is made to provide some constraint on gluon distributions, $G(x)$. Theoretically one expects scale sensitivities to cancel in the ratio; experimentally, the uncertainty in luminosity \mathcal{L} cancels. The ratio, as shown in Fig. 5, is plotted as a function of $x_T = 2E_T^2/\sqrt{s}$, which is the fraction of E_T available for photon production.

The ratio is in good agreement with NLO QCD for $E_T > 36$ GeV, but tends to lie below the prediction for $E_T < 36$ GeV ($x_T \leq 0.04$). The systematic error is the quadrature sum of the individual cross sections, and is dominated by purity uncertainties. Due to the magnitude of the uncertainties, nothing conclusive can be said about $G(x)$, for $x_T \leq 0.04$.

CDF preliminary forward photon measurement of $d\sigma/d\eta$ is shown in Fig. 6. For this analysis the events were selected in the forward plug calorimeter with a cone radius $\mathcal{R} = 0.7$, an isolation cone $E_T < 3$ GeV, and with photons candidates restricted to $1.32 < |\eta| < 2.22$. Central photons were required to be within $|\eta| < 1.0$. For the measurement the photon transverse energies were integrated over the range $27 < E_T < 40$ GeV. Though the theoretical curve is in qualitative agreement with the data, the systematic errors preclude one from distinguishing between pdfs.

3.3 Photon + Jets

The CDF photon + 2 jets¹² measurement is motivated by its hope of making a distinction between direct photon production and bremsstrahlung. In Comp-

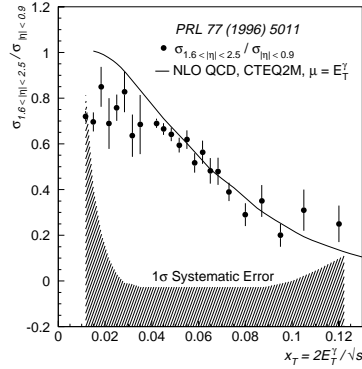


Figure 5. $D\bar{O}$ ratio of forward to central inclusive photon cross sections

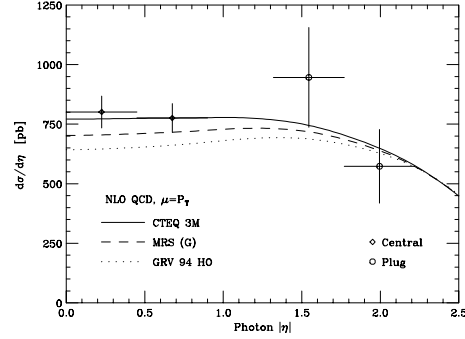


Figure 6. CDF cross section as a function of η .

ton(annihilation) processes, gluons can be radiated by the final state quark(gluon). A bremsstrahlung photon might be radiated in a $qg \rightarrow qg$ process with the q radiating the photon to yield the same final $\gamma + 2jet$ final state.

CDF required a photon with $|\eta| < 0.9$ and $E_T^\gamma > 16$ GeV and 2 jets with $|\eta| < 2.5$ and $E_T^{jet} > 8$ GeV. Background subtraction yields insight into Double Parton Scattering, DPS . The DPS contribution was estimated by overlaying uncorrelated low E_T jet events with inclusive photon events and comparing these events to the data. Fig. 7 shows the $\Delta\phi = (\phi_\gamma + \phi_{jet1}) - \phi_{jet2}$ distribution. Correlated events are expected to peak near π , whereas uncorrelated events would yield a flat distribution. The resulting DPS background from 16pb^{-1} of data was determined to be $14_{-7}^{+8}\%$.

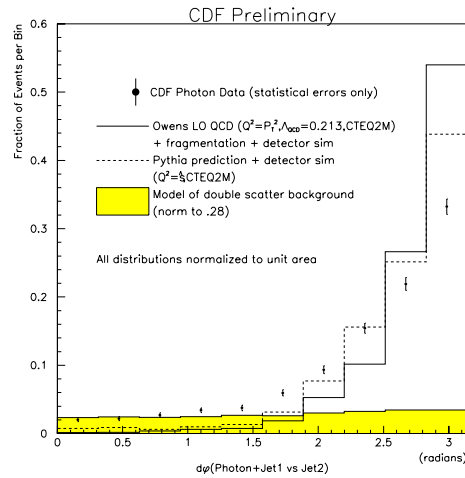


Figure 7. $\Delta\phi = (\phi_\gamma + \phi_{jet1}) - \phi_{jet2}$ Theory: Tree Level \rightarrow NLO + Fragmentation (solid) Theory: Pythia \rightarrow LO + Parton Showers + DPS (dashed)

Fig. 8 and Fig. 9 show the kinematic and angular distributions. The data are

compared to tree level, TL , $2 \rightarrow 3$ prediction which includes parton fragmentation and detector simulation, and Pythia $2 \rightarrow 2$ predictions with parton showers. In Fig. 8 the 3 body mass spectrum predictions are in agreement with the data. Also in the figure, one sees that both models predict a harder photon E_T spectrum than is seen in the data; this is consistent with $D\phi$ and CDF inclusive photon measurements. The predicted TL jet E_T spectra are harder than the data, while within experimental uncertainties, the Pythia predictions are more consistent.

To estimate the bremsstrahlung component of the total inclusive photon cross section, the angular data were fit to normalized Pythia generated pure direct photon and pure bremsstrahlung photon azimuthal distributions. The fit results in a bremsstrahlung component of $(55 \pm 15_{-10}^{+5})\%$, where the 15% is the statistical error and the systematic error is estimated by varying the kinematic distributions within known systematic uncertainties.

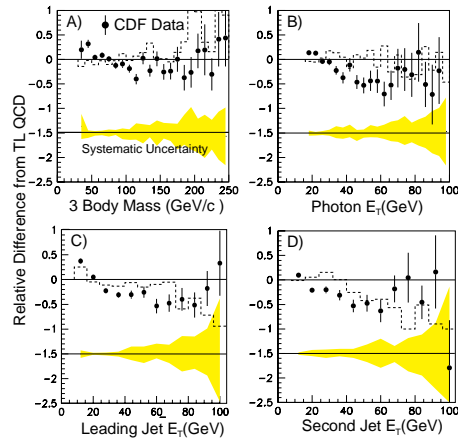


Figure 8. CDF $\gamma + 2jet$ events: 3 body mass and E_T^γ , E_T^{jet1} , E_T^{jet2} distributions. Points are $(data-TL)/TL$ and dashed line is $(Pythia-TL)/TL$.

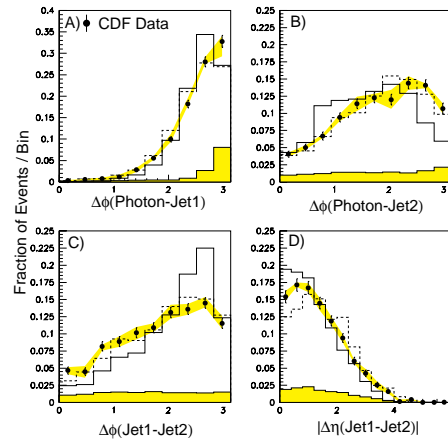


Figure 9. CDF $\gamma + 2jet$ events: Angular distributions. The DPS subtracted background is shown as the shaded region at the bottom of each plot.

3.4 CDF Photon + Muon

A new measurement from CDF measures the charm content of the proton. The process is Compton $\gamma + charm$ scattering. Only one calculation exists to date which is a NLO calculation by B. Bailey, E. Berger, and L. Gordon¹³. This prediction lacks the expected 25–30% $\gamma + b$ contribution which is present in Pythia. NLO corrections are large due to processes such as $gg \rightarrow c\bar{c} \rightarrow c\bar{c} + \gamma$, where a c -quark radiates a photon.

Fig. 10 shows that the dominant background to this process is decays-in-flight of pions and kaons. Fig. 11 shows the measured cross section and compares it to the NLO QCD prediction of Gordon and Berger, and Pythia predictions of $\gamma + c$, $\gamma + b$, $\gamma + c, b$. Though the measurement errors are large, they do favor the NLO QCD prediction and require both c and b contributions from Pythia.

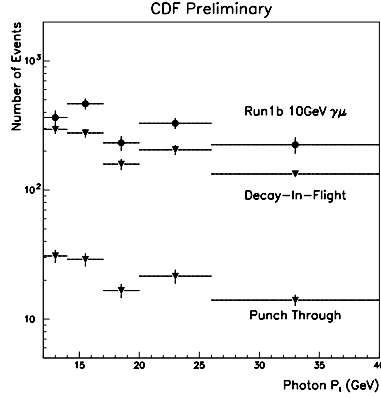


Figure 10. CDF components of $\gamma + \mu$ signal.

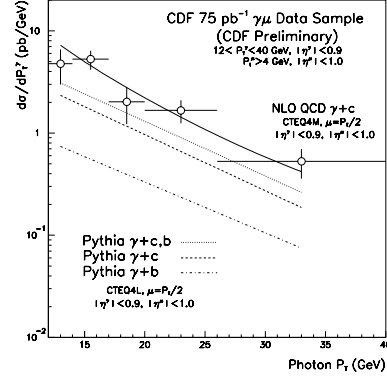


Figure 11. CDF $\gamma + \mu$ cross section

4 Di-Photon Results

Despite the low cross section, di-photons provide a powerful tool for studying QCD due to the relative ease of measuring photon positions and energies, and the avoidance of jet ambiguities. A measurement of the vector sum of di-photon momentum, or $k_T = |\vec{p}_T^1 + \vec{p}_T^2|$, provides a direct measurement of the parton intrinsic transverse momentum.

Fig. 12 shows a comparison of DØ and CDF measurements of the photon E_T spectrum, vector sum of transverse momenta, the photon azimuthal difference, and the di-photon invariant mass. In each plot, the experimental measurements are consistent. In Fig. 13, the DØ preliminary k_T measurement is compared to NLO QCD², Pythia³, and RESBOS resummation⁴. RESBOS and Pythia show good agreement with the data, though the data is harder than each prediction for $k_T > 35$ GeV. NLO QCD agrees with the data above $k_T > 5$ GeV, but deviates at lower intrinsic momentum.

5 Summary and Conclusions

Both DØ and CDF measurements are consistent and complementary. For the inclusive cross section measurements, both experiments agree with NLO QCD for $E_T \gtrsim 30$ GeV, while both lie above theory at lower E_T . Both experiments have made measurements in the forward pseudo-rapidity regions, however experimental uncertainties preclude these present measurements from discriminating between pdfs. CDF's $\gamma + 2jet + X$ measurements estimates a double parton scattering level of 14%; additionally, the measurement yields the bremsstrahlung contribution to direct photon production at the level of 55%. CDF has also contributed to knowledge of the charm contribution of the proton with its $\gamma + \mu$ cross section measurement.

DØ and CDF have also measured di-photon production. Both experimental measurements are consistent over the ranges probed. DØ has also compared its

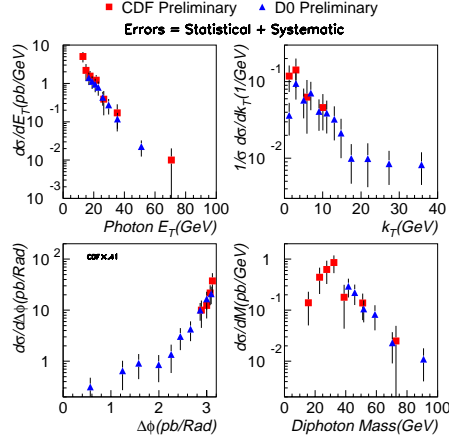


Figure 12. CDF and DØ Di-Photon Results: top left: photon E_T ; top right: vector sum of transverse momentum; lower left: photon azimuthal difference; lower right: di-photon invariant mass

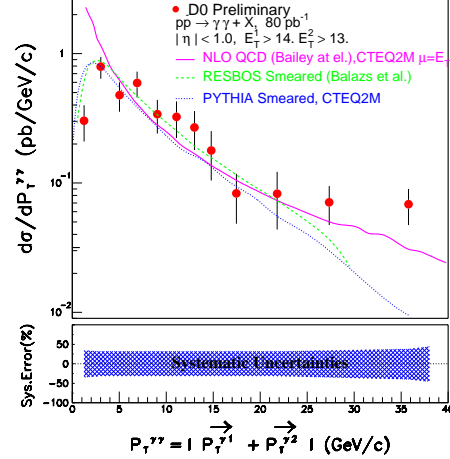


Figure 13. DØ Di-Photon vector sum of transverse momenta: the data (points) are compared to Pythia parton showers (solid), Resummation (dotted), and NLO QCD (dashed).

intrinsic k_T measurement with NLO QCD, Pythia, and RESBOS resummation. Both RESBOS and Pythia show good agreement with the data for $k_T \leq 25$ GeV, but are softer than the data above 25 GeV; NLO QCD predictions are consistent with the data above 5 GeV, but the theory diverges at lower k_T .

While QCD gives a good overall description of direct photon production, there still exist numerous discrepancies between experiment and theory. Thus photons continue to be a fruitful arena for QCD.

References

1. T.Ferbel and W.R.Molzon, *Rev. Mod. Phys.* **56**(1984) 181.
2. B.Bailey,J.F.Owens,and J.Ohnemus, *Phys. Rev.* **D46** (1992) 2018.
3. T.Sjostrand et al., *PYTHIA 5.7 and JETSET 7.4 Physics Manual* (1993m revised 1994) **CERN-TH.7112/93**
4. C.Balazs and C.P.Yuan, *hep-ph/9704258*.
5. L.Apanasevich et al., *hep-ph/9808467*.
6. S.Abachi et al., *Nucl. Instr. and Meth.* **A338**(1994)185.
7. F.Abe et al., *Nucl. Instr. and Meth.* **A271**(1988) 387.
8. F.Abe et al., *Phys. Rev. Lett.* **73**(1994) 2662.
9. H.L.Lai et al., *Phys. Rev.* **D55**(1997) 1280.
10. CTEQ internal report (unpublished).
11. S.Abachi et al., *Phys. Rev. Lett.* **77**(1996) 5011.
12. F.Abe et al., *Phys. Rev.* **D57**(1998) 67.
13. B.Bailey, E.Berger, and L.Gordon, *hep-ph/9608431*.